Time-resolved detection of luminescence for electrophoretic methods

Bryan J. Dodgson, Sergey N. Krylov

Time-resolved luminescence has been employed as a method of detection for electrophoretic studies for nearly two decades. We discuss experiments conducted on capillary-zone electrophoresis, capillary-gel electrophoresis, slab-gel electrophoresis and microchip electrophoresis. We place emphasis on the variety of sample molecules, and applications in order to show the versatility of this technique.

Keywords: Capillary-gel electrophoresis; Capillary-zone electrophoresis; Electrophoresis; Excitation wavelength; Fluorescence; Instrumentation design; Limit of detection; Microchip electrophoresis; Slab-gel electrophoresis; Time-resolved detection

Bryan J. Dodgson, Sergey N. Krylov*
Department of Chemistry and Centre for Research on Biomolecular Interactions, York University, Toronto, Canada

*Corresponding author.
Tel.: +1 416 736 2100x22345;
Fax: +1 416 736 5936;
E-mail: skrylov@yorku.ca

1. Introduction

Capillary electrophoresis (CE) is a powerful analytical tool capable of separating chemical species by charge-to-size ratios. It has found a variety of uses in the analytical sciences, including not only classical separation and purification of chemical species, but also determining the kinetic parameters of reactions [1–5], affinity-based selection of ligands [6–9], single-cell analysis [10–13] and as a microreactor platform [14–17]. The modes of detection for CE include absorption, fluorescence, electrochemical (amperometric) and index of refraction-based methods [18]. Within these modes, laser-induced fluorescence (LIF) detection is the most sensitive, as customized CE-LIF set-ups have been capable of achieving limits of detection (LODs) as low as 50 yoctomol (10^{-24} mol), corresponding to single-molecule detection [19].

Despite its sensitivity, LIF detection has some disadvantages: natural and unpurified samples can display high levels of scattering, and non-specific fluorescence that increases background and reduces sensitivity. Multiplexing by LIF requires multiple light sources and detectors that can be expensive and difficult to align [20]. CE-LIF set-ups able to achieve low LODs use off-column detection to reduce reflections at the capillary walls, but the sheath-flow systems used in these set-ups are difficult to set up and to maintain [21] and are unable to perform some of the CE protocols designed using on-column commercial instruments (i.e. off-column collection or running the sample back through the detection window).

Time-resolved (TR)-detection methods are used to measure fluorescence intensity as a function of time following a brief pulse of excitation light. Coupling TR detection to CE-LIF can solve many of the problems listed above. A major impediment to sensitivity with CE is the background signal from scattering, which can occur at wavelengths different from (Raman scattering) or directly at (Rayleigh scattering) the wavelength of the laser. While spectral filters can be ineffective against high-intensity Rayleigh scattering and Raman scattering at the wavelength of fluorescence, TR measurements can discriminate scattering from fluorescence (and other luminescent processes), since the two occur on different timescales. TR measurements can also be used to discriminate between different fluorescent species emitting at the same wavelength based on characteristic lifetime profiles. TR detection has been used to improve the sensitivity of CE, filter short-lived scattering and fluorescence from complex samples and

0165-9936/$ - see front matter © 2012 Elsevier Ltd. All rights reserved. doi:10.1016/j.trac.2011.10.007

provide a means to identify peaks and to perform multiplexing by lifetime.

It has been over a decade since the last review on the subject of TR-CE [22], which covered only experiments using near-infrared (NIR) detection. This review covers a wide variety of electrophoretic experiments using TR luminescence-measurement techniques. We highlight the difficulties and the benefits of TR-CE, as well as the equipment necessary for its implementation. We also assess the merits of this technique and discuss future applications.

2. Time-resolved measurements

2.1. Non-lifetime

TR detection can be used to acquire the fluorescence intensity within a well-defined window following a pulse of excitation light. This is the time-gated mode of detection. An integrated measurement is performed only within a specific window that is defined by its duration (gate width) and start time relative to pulse arrival (delay time). There is no temporal resolution between photons detected within the gate, so lifetime information can be determined only if multiple gates are used per excitation cycle. If the correct delay time and gate width are chosen, photons originating from processes occurring earlier, or later, than the process of interest can be rejected. In this way, time gating can be used as a method of temporal filtering to decrease the noise of the system.

2.2. Time domain

Lifetime measurements can be made in the time domain (TD) using short pulses of excitation and detection equipment with sufficient time resolution to measure the intensity of fluorescence distinctly as a function of time following the excitation pulse. Repeated excitation of the sample is required to construct an accurate lifetime profile. By fitting the curve to a model, the fluorescent lifetime parameter(s) can be determined.

2.3. Frequency domain

Lifetime measurements can also be made in the frequency domain (FD) by periodically modulating the intensity of the excitation source and measuring the resulting phase and amplitude shift of the modulated fluorescence signal. The phase and amplitude shift, measured over a range of modulation frequencies, can be Fourier transformed to give the fluorescence-intensity-decay curve in the time domain. From this curve, the lifetime data can be determined.

Both methods of lifetime determination have their advantages. In general, FD methods are considered more accurate for determining lifetimes with multi-exponential behavior [23]. However, it has been shown that TD methods produce greater accuracies for single exponential lifetime measurements [24]. This is due to the long dark periods of data acquisition in the TD mode, which are free from the noise of photon-detection statistics.

A more detailed description of each method is given in the respective chapters in Lakowicz's book on fluorescence spectroscopy [25].

3. Challenges of time-resolved electrophoresis

3.1. Focusing geometry

TR measurements performed in a small channel or capillary can introduce problems not normally encountered when studying samples in a cuvette or on a coverslip. The curvature of a capillary can increase reflections and the confined sample volume can impose restrictions on the size of the detection volume. Two popular optical configurations used for a TR-CE instrument are shown in Fig. 1. The dual lens set-up uses separate lenses for focusing and collecting light. The two lenses are commonly placed at 90° to minimize the amount of scattered light that is collected, however an angle near 56° (Brewster's angle) has also been used [26–28]. Brewster's angle eliminates the reflection of p-polarized light and is used on systems with large, flat surfaces {e.g., slab gels [26], microchips [27] and microanalysis plates [28]}. The single lens set-up uses the same lens for focusing and collecting, along with a dichroic filter to direct excitation and fluorescent light in different directions. A significant amount of backscattering may reach the detector in this set-up, so confocal optics is often used to filter the light spatially in the direction of beam propagation. Briefly, confocal optics focuses the collected light to a point at a pinhole aperture. The aperture rejects light collected from outside the focal plane of the lens (i.e. scattered light from capillary walls) [29].

The capillaries used in the literature had inner diameters of 50–200 μm. Focal spot sizes were generally made much smaller than this, using 10–65 times magnification objectives with numerical apertures (NA) less than 0.85. Recorded detection volumes were in the range sub-pL–nL, and smaller detection volumes were avoided in the interests of detecting the greatest number of molecules passing through the capillary. One study performed electrophoresis in a cone-shaped microcapillary, with an inner diameter of 0.5 μm at the outlet. A small detection volume was used and nearly all molecules exiting the capillary could still be detected [30]. Confocal optics and a $100\times$ oil immersion objective (NA = 1.4) were used to create the small detection volume, which was made slightly larger than the capillary outlet (greater than 0.5 μm in diameter).

The use of a pulsed UV LED as the excitation source introduced some difficulties in focusing [31]. LED

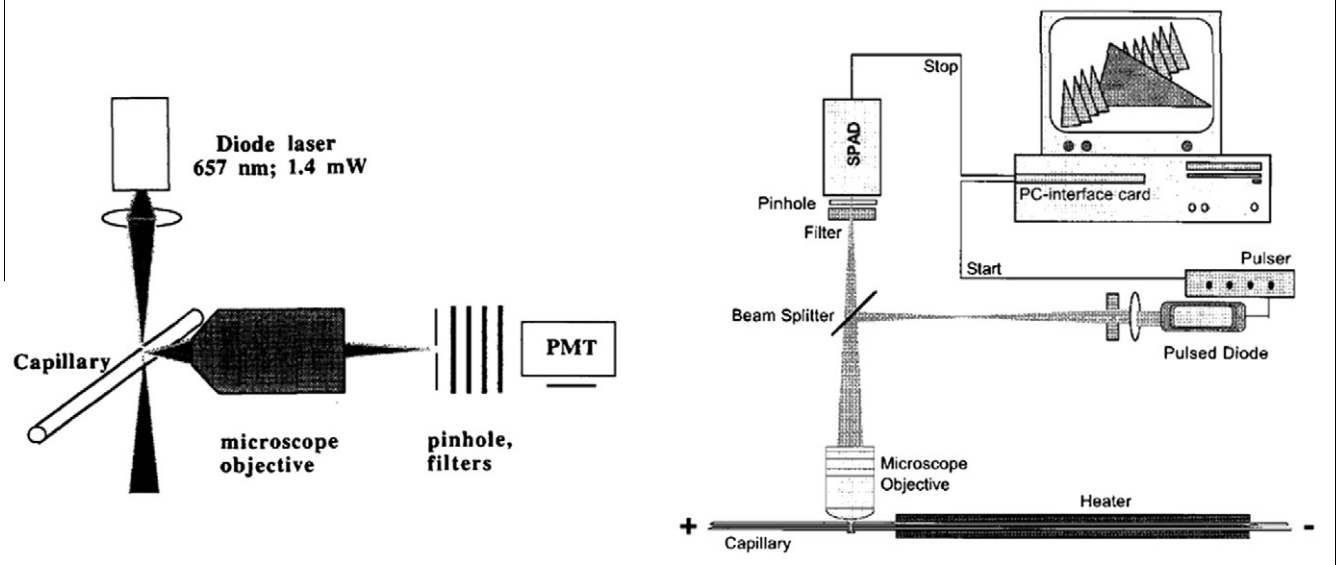

Figure 1. Schematic examples of 90 ° dual lens configuration (left), and single lens configuration (right). Reprinted from [37] and [49] with permission from Elsevier and the American Chemical Society respectively.

emission is non-coherent and non-monochromatic, so the light had to be collimated and filtered before being focused into the capillary. The system was not thoroughly optimized and it was speculated that further tuning of the optical design may increase the overall LOD of the system.

A study by Zhu et al. used two beams of different wavelengths to perform TR-CE on a microfabricated glass device [32]. The different indexes of refraction for the two wavelengths resulted in two spatially separated focal spots. In addition, the thickness of the chip's cover plate also prevented proper focusing. Despite careful alignment of the system, focal aberrations and collection inefficiencies were expected to limit sensitivity.

Li and McGown performed lifetime determinations in the frequency domain by integrating a commercial multi-harmonic Fourier-transform instrument with a commercial CE system [33]. Different alignment designs were tested using various filter and lens combinations with each design. In a later study, they revisited their set-up by testing two dual-lens configurations (120° and 90°) and one single-lens configuration. Using a variety of filters, objectives and capillaries, they were able to find the conditions giving the greatest sensitivity [34].

Difficulties of focusing optics and geometries were completely circumvented by Fultz et al., who delivered in-column axial excitation by inserting a 100-μm optical fiber into a 200-μm inner diameter capillary [35]. A spectral filter in front of the detection window was the only optical component used.

3.2. Residence time

The mobilities introduced by electrophoresis place limitations on the maximum number of photons that can be collected from a single electrophoretic band of molecules. The statistical nature of photon emission implies that the accuracy of lifetime determination is reduced as fewer photons are collected. The studies reviewed here make single lifetime measurements from data collected in second-long intervals or by averaging multiple lifetime measurements made from data collected in millisecond-long intervals. A variable integration time was used by Soper et al. by defining a collection interval that began and ended when the signal crossed a threshold value 25% above the average background count rate [36]. In this way, integration times as long as 9 s were achieved.

To make an exact lifetime measurement, 10^4 photons should be detected in the maximum channel and 10^5–10^6 photons over all channels [37]. It is difficult to detect this many photons in the short integration times discussed above, so lifetimes are often determined using data-fitting algorithms. Non-linear least squares (NLLS) is a common data-fitting method, but it uses the assumption that errors follow a normal distribution. Photon-arrival times (hence photon detection) are governed by Poisson statistics, which deviates from a normal distribution at low counts. Because of this, NLLS is inaccurate for short collection times. A more accurate method is maximum likelihood estimators (MLE), which is derived using an assumption that errors follow a Poisson distribution. It is given by the following equation [38]:

$$1 + (e^{T/\tau} - 1)^{-1} - m(e^{mT/\tau} - 1)^{-1} = N_t^{-1} \sum_{i=1}^{m} iN_i \qquad (1)$$

where T is the width of each time bin, m is the number of time bins per decay profile, N_i is the number of photon counts in bin i, N_t is the total number of counts in the

decay and τ is the lifetime parameter that is being sought. Derivation of this formula is discussed elsewhere [39].

The superiority of MLE over NLLS has been confirmed experimentally by collecting photons from dyes in a polymer film [40]. It was found that, when less than 2×10^4 photons were detected, NLLS underestimated the fluorescent lifetime by ~5%. With fewer than 10^3 photons, NLLS gave unreasonable results. When more than 2×10^4 photons were collected, NLLS converged to the results of MLE, which were stable over the whole range of intensities. However, MLE inherently assumes a mono-exponential decay function and this can lead to inaccurate results if the lifetime is multi-exponential [40].

Bachteler et al. improved on the MLE method by using a pattern-recognition technique. In their technique, lifetime data was acquired for each dye in a separate calibration experiment, and then fitted to lifetime data from a TR-CE separation using MLE [37]. Each peak was identified based on the set of calibration data to which it best fit. With this method, only 800 photons were needed to determine lifetimes with 90% accuracy and fewer than 10^4 total photons were estimated to be needed for exact identification.

The method of rapid lifetime determination (RLD) was used in a single study [36], but it was found to be less accurate than MLE at low concentrations. Frequency-domain lifetime determinations used continuous excitation, so a large number of photons were detected, making NLLS reliable. In addition, the frequency-domain techniques used the maximum-entropy method (MEM) to find the best model to use in the NLLS fitting (i.e. the number of exponential decays) [33]. For most experiments, MLE was the method of choice for lifetime determination.

4. Instrumentation

4.1. Excitation source

A non-steady state light source is required to make TR luminescence measurements. In the time domain, a short pulse of excitation light is used, whereas measurements in the frequency-domain require an intensity-modulated excitation source. A short excitation pulse (shorter than the lifetime) is desirable for time-domain measurements, as it ensures most molecules are in the excited state when the pulse ends. In the frequency domain, a range of modulation frequencies should be used to measure the fast and slow parts of the decay curve.

4.1.1. Laser. Lasers are the preferred source of excitation light due to the coherent, monochromatic and high-intensity light that they emit. Lasers are also capable of producing short and stable pulses, which are necessary for time-domain measurements. Table 1 gives a list of the lasers used in the literature. The headings of the columns in Table 1 are relevant to TR measurements for the following reasons:

(1) the emission line defines which dyes can be excited;
(2) the pulse width defines the lower limit of dye lifetime that can be accurately measured;
(3) the repetition rate limits the number of collected photons, so it should be as high as possible while still allowing for complete decay between pulses; and,
(4) the laser power should be high enough to saturate the sample, as beams are easily attenuated but not so easily intensified.

The most common lasers used in the literature were pulsed semiconductor (or diode) lasers. The wavelength range of these lasers was in the red or NIR region because these lasers operate best at these wavelengths, and because scattering is reduced in this region. Pulsed semiconductor lasers are also favored for their simplicity of use (i.e. turn-key operation), compact design, wide variety of available wavelengths and affordable cost. However, diode heads that emit in the green region of the spectrum are difficult to obtain, and, for all diode lasers, care must be taken to account for the broad spectral width of the pulse (up to 10 nm) and the elliptical shape of the beam profile.

4.1.2. Non-coherent light sources. Lasers are one of the most expensive components of a CE-LIF instrument and alternative sources of pulsed excitation have been investigated. LEDs are an attractive alternative, as they have longer lifetimes than lasers, and are cheaper, smaller, and easier to operate.

Hillebrand et al. employed a pulsed UV-LED for excitation [31]. The LED had a center wavelength of 370 nm, a spectral width of 12 nm and a repetition rate of 500 Hz, but the pulse width was never characterized. The pulsed LED used by Lammers et al. emitted at 465 nm with 300-μs pulses and a repetition rate of 230 Hz [52].

Xenon flash lamps have also found use as an excitation source for TR-CE studies, as part of a commercial luminescence detector [53] or a custom-designed assembly. A 15-W Xenon flash lamp operated at 1 μW/cm^2, with a repetition rate of 500 Hz and a band pass filter centered at 350 nm, was used in a custom-designed set-up [54,55]. The microsecond pulses of flash lamps make them useful for studies of long-lived luminescence.

4.2. Detector

For a detector to be used in a TR set-up, it must exhibit better temporal resolution than the lifetime of the molecule being studied. In addition, the small dimensions of the detection volume in CE favor point detectors over imaging ones. These two requirements make fast-response photomultiplier tubes (PMTs) and single-photon

Table 1. Description of lasers used in time-resolved (TR) electrophoretic methods

Laser Type	Emission line	Pulse width	Repetition rate	Average power	Other details	Ref.
Nd:YLF	349 nm	2.5 ns	2 kHz	1.9 mW	Prototype laser with 18% pulse-to-pulse standard deviation in energy	[41,42]
Ti:Sapphire	830 nm	120 fs	76 MHz	12 mW	Passively mode locked, pumped by argon-ion laser	[36,43]
Nd:YAG	532 nm	9 ns	10 Hz	1 mW	Q-switched pulsing	[35]
Nitrogen gas	337 nm	500 ps	100 Hz	Not given	Laboratory-made	[44]
Excimer-pumped dye laser	280, 290, 321 nm	15 ns	10 Hz	25 mW	XeCl gas in the excimer laser	[45]
Diode pumped UV	266 nm	10 ps	40 MHz	30 mW	Mode-locked pulsing	[46]
Argon ion	488, 514 nm	NA	NA	100 mW (max. power)	Intensity was sinusoidally modulated with a Pockells cell for FD measurements	[33]
Pulsed semi-conductor	655–780 nm	74–500 ps	3.8–80 MHz	~1 mW	A variety of these lasers were used in the literature, individual laser specs fell within the given ranges	[27,30,32,37,47]

avalanche photodiodes (SPADs) the detectors of choice for TR measurements. Through different mechanisms, these detectors produce a measureable current following the detection of one, or many, photon(s). For a more technical review of each detector, the following references should be consulted for PMTs [56] and SPADs [57]. In general, PMTs provide larger photoactive areas and lower after-pulsing probabilities, while SPADs provide higher detection efficiencies and lower dark noise. The photoactive area of a SPAD is typically a few hundred micrometers in size, which must be accounted for in the optical alignment of the system.

4.2.1. Detection mode. TR measurements can be made in analog or digital (photon-counting) mode.

In analog detection, the current produced in the detector by the arrival of photons is integrated over time. The inherent noise of the instruments and the photomultiplication process is added to the Poissonian noise of photon-arrival statistics (shot noise).

In digital detection, a threshold current is defined and, whenever a pulse exceeds the threshold, a photon is counted. The threshold is set above the noise of the instruments and below the current produced by a single photon, and this allows digital detection to better approach the shot noise limit of photon detection. The digital mode does not discriminate between detection of multiple and single photons, so it operates on the assumption that no more than 1 photon arrives within the temporal resolution of the detector. This assumption makes single-photon counting useful in low-intensity detection ranges (i.e. when count rates are less than 10^6 Hz). Digital photon counting requires advanced instrumentation, but this equipment is often available in compact electronics boards.

For the determination of fluorescent lifetimes, time-correlated single-photon counting (TCSPC) is used. For each photon that is detected, TCSPC measures the time between the excitation pulse and the detection of that photon. A histogram of these times is built up over many excitation cycles to reconstruct the fluorescence-decay curve. A more detailed explanation on TCSPC and the instrumentation necessary for its use is given elsewhere [58].

4.3. Instrument-response function

Each piece of equipment necessary for TR measurements (excitation source, optics, sample, detector and data processor) processes photons with a distribution of times, which is compounded and the end result is known as the instrument-response function (IRF). The IRF is determined by measuring the temporal profile of an ''instantaneous'' process and the width of the IRF defines the minimum lifetime that an instrument is capable of measuring.

One of the first TR-CE instruments had an IRF of 8 ns, which forced the authors to use a longer lifetime dye (16 ns) despite its poor photophysical characteristics [41].

An IRF in the microsecond range was achieved using a Xenon flash lamp and a photon-counting PMT to study long-lived luminescence from lanthanide chelates [54,55].

An IRF of hundreds of microseconds was used to study the lifetime of phosphorescence on CE using a pulsed LED and an analog PMT [52].

The shortest IRF measured in a TR electrophoretic study was 165 ps using a Ti:sapphire laser and a SPAD detector with TCSPC capabilities [36].

Studies using pulsed semiconductor-diode lasers were able to achieve IRFs as low as 275 ps [59], but on average IRFs between 500 ps and 1 ns were recorded.

5. Applications

The literature on TR electrophoretic studies shows two implementations of this method: time gating and lifetime determination. Data collected in the lifetime-determination mode can always be time gated, but generally the reverse is not true. The extra information provided by lifetime-determination experiments comes at the expense of increased equipment cost and complexity.

5.1. Time gating

5.1.1. Analysis of highly contaminated samples. Time gating is useful for experiments that suffer from poor sensitivity and low LODs [e.g., the analysis of complex biological or environmental samples like serum, urine, cell lysate, waste or natural water samples]. These samples contain a variety of chemical species that may fluoresce near the wavelength of interest or contribute to high levels of scattering.

Miller and Lytle used time-gated CE-LIF to detect the UV dyes 4-MBNA and 2,5 Dns-Cl spiked into samples of urine and *E. coli* supernatant [41]. The dyes had 20-ns lifetimes, so short-lived fluorescence and scattering could be gated out, but both dyes had poor molar absorptivity. A concentration LOD of 1 nM was obtained, which was three orders of magnitude better than absorbance detection.

Fig. 2 shows the experimental results of a diluted sample of human urine spiked with 500 nM of 2,5 Dns-isoleucine and analyzed using two time-gating scenarios: 0 ns delay with a 10 ns width, and 60 ns delay with a 50 ns width. The dye was difficult to distinguish from the background in the first scenario, but became the sole prominent peak in the second. The same procedure was repeated for 300 nM of 4-MBNA spiked in diluted *E. coli* supernatant, with similar results. The same group performed enzyme assays in CE using leucine aminopeptidase (LAP), which created a fluorescent product upon cleaving leucine from the non-flourescent L-leucine-4-MBNA molecule [42]. LAP was detected in human serum, dialyzed urine and *E. coli* supernatant and an LOD of 400 molecules was estimated.

Kok et al. analyzed river-water samples for the signature native fluorescent signal from naphthalene sulfonates, which absorb in the UV range and have lifetimes of under 10 ns [45]. Pulsed and continuous wave (cw) UV lasers were used. Pulse widths of 15 ns at repetition rates of 10 Hz were achieved in pulsed mode. The laser's poor performance characteristics prevented TR detection from being more sensitive than cw detection when

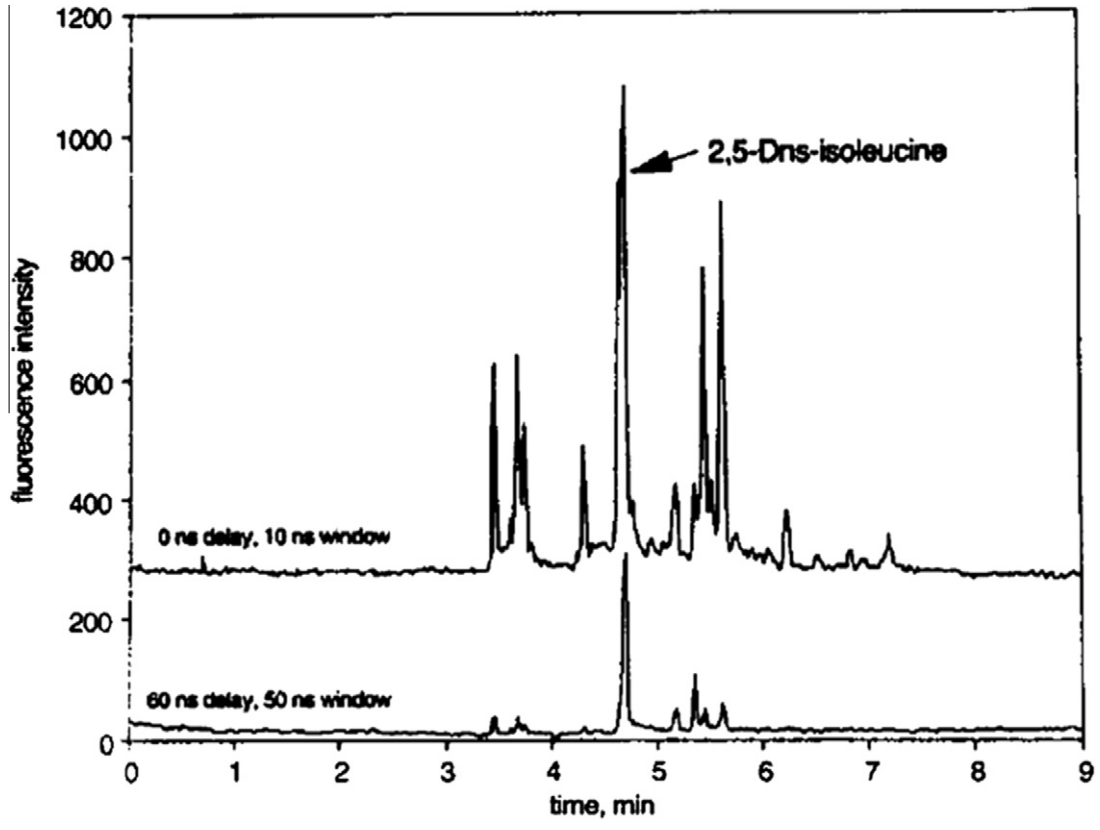

Figure 2. Electropherograms for 1:200 dilution of human urine sample spiked with 5×10^{-7} M 2,5-Dns-isoleucine. Data were collected simultaneously using two different integration delays and windows. Data have been offset for clarity [41].

analyzing samples of pure sulfonates. However, when river-water samples were analyzed (following off-line solid-phase extraction) TR detection proved to be just as good, or better, than the steady-state mode. No delay time was employed for the measurements, but a 30-ns gate-width was used to reject long-lived fluorescence and dark noise.

5.1.2. Analysis of proteins. By performing in-axial excitation *via* an optical fiber inserted in the capillary, Fultz, Branch and Majidi performed CZE analysis of two rhodamine-conjugated proteins, bovine-serum albumin (BSA) and horseradish peroxidase [35]. The data was processed using a variety of time delays between 275 ns and 2000 ns (sic). The LOD of free rhodamine dye was measured to be 19 fmol, a five-fold improvement from the LOD on the same system using cw detection. While the LODs of specific proteins were not given, it was claimed that LODs were in the fmol range.

Using a pulsed UV LED, Hillebrand et al. studied fluorescamine-derivitized bradykinin, lysine, keratinase, serine and aspartic acid in a single run of CE. By optimizing the delay time, gate width and repetition rate of the laser, LODs of 3 fmol and 18 fmol were achieved for bradykinin and lysine, respectively [31].

Belin and Seeger developed a MiniCE device (10-cm long capillary) that used a pulsed UV laser to study native fluorescence from lysozyme and beta-galactosidase [46]. Using confocal detection and short laser-pulse widths (<10 ps), they performed on-line TCSPC measurements during the separation of three proteins (lysozyme, β-galactosidase and BSA). They made no mention of optimizing the TR aspect of their instrument. An LOD is not given in terms of number of molecules, but concentration limits of 9.0 fg/μL (600 pM), 13.0 fg/μL (200 pM) and 55 fg/μL (500 pM) were reported for lysozyme, β-galactosidase and BSA, respectively. This represents a 100–1000 times improvement from the LODs achieved by PAA gel electrophoresis. With this method, the authors claim to have achieved the lowest LODs for proteins in the literature.

5.1.3. Analysis of long-lifetime species. The study of species with long lifetimes is favored by the slower time response of many time-gated TR-CE instruments. Lanthanide chelates have millisecond-long luminescence lifetimes and are prime candidates for TR-CE.

One of the first experiments to use TR-CE measured the indirect signal from nitrites in an environmental sample through quenching a terbium(III) chelate present in the run buffer [53]. A commercial luminescence detector with a delay time of 0.1 ms and a gate-width of 0.5 ms was used, and a concentration LOD of 200 nM was achieved. A sample of tap water spiked with nitrites was also analyzed and LODs were superior to other techniques.

Latva et al. studied two europium(III) chelates with lifetimes of 394 μs and 905 μs by coupling a luminescence detector to the capillary of a CE apparatus [44]. Using a delay time of 100 μs and a gate-width of 1.0 ms, concentrations down to 100 nM were successfully measured.

Sumitomo et al. developed a chelate label that was stable under the high EDTA/phosphate, high-heat and high-voltage conditions found in CE assays of DNA and proteins [54]. Using a Xenon flash lamp and a photon-counting PMT, the chelate was labeled to a single-stranded DNA probe and used in a hybridization assay. The lifetime of the chelate was 1.19 ms and a delay time of 100 μs was used to filter all the data temporally. The hybridization experiment was successfully performed in both pure buffer and a sample of fetal bovine serum. The same group also studied the separation of five proteins labeled with the chelate (lysozyme, β-lactoglobulin, trypsinogen, ovalbumin and BSA) [55]. All five proteins were separated by CGE in proportion to their molecular weight and with LODs better than UV absorption. An equivalent separation experiment was performed in a solution of BSA, and the LODs were nearly unchanged.

5.2. Lifetime determination

5.2.1. Identification and multiplexing by lifetime. Motivation towards lifetime determination in CE was driven by the need for multiplexing in a CE experiment. Although spectral multiplexing was well developed [60–62], it was understood to be technically difficult due to the different excitation sources and detectors needed as well as the cross-talk between spectral channels [49]. TR-CE allowed for dyes to be identified and multiplexed by differences in their fluorescent lifetimes.

Bachteler et al. separated and identified two NIR dyes with lifetimes of 1.1 ns and 2.4 ns with an accuracy of 91% [37]. Soper et al. performed a similar work identifying two dyes with lifetimes of 481 ps and 936 ps [36]. Their instrumentation allowed for lifetimes to be determined with a high accuracy (<30 ps) and they extended their system to separation and identification of six dyes by lifetime.

Zander et al. used lifetime determination to identify single molecules exiting a tapered microcapillary [30]. The detection volume was aligned at the capillary outlet (0.5 μm) and fluorescent bursts were detected from individual molecules as they exited the capillary. Lifetime measurements were made from TR analysis of the bursts. The accuracy of lifetime determination allowed for 80% correct identification between the two dye-labeled mononucleotides studied: Cy5-dCTP, with a lifetime of 1.4 ns; and, JA53-dUTP, with a lifetime of 2.5 ns. This set-up also allowed for the determination of molecular diffusion times from the photon-burst statistics.

Recent work by Lammers et al. used TR phosphorescence to identify enantiomers of chiral compounds. Enantiomers of camphorquinone were separated in CE by placing chiral α-cyclodextrin, which preferentially associates to one enantiomer, in the run buffer [52]. The phosphorescent lifetimes of the enantiomers were also affected by association with the chiral compound, and lifetimes of 384 μs and 144 μs were observed for the (+) and (−) enantiomers, respectively. Excitation was provided by a pulsed LED at 465 nm capable of emitting 300 μs pulses with a repetition rate of 230 Hz. Photon collection began 10 μs after the LED pulse and a PMT measured the intensity in 2-μs bins over 1024 μs. A sub-μM concentration LOD was achieved for the two enantiomers.

The concentration LOD was improved to 200 nM using a sensitized phosphorescence-detection system with bupropion as the enantiomer and a pulsed UV laser for excitation [63]. Applying the sensitized detection method to the camphorquinone and α-cyclodextrin system provided LODs of 50 nM for both enantiomers and lifetime values of 238 μs and 126 μs for the (+) and (−) enantiomers, respectively [64]. This technique was proposed as a method to determine the concentration of enantiomers leaching into water from a cured dental resin, as well as for the study of other chiral systems. The same methodology was then applied to separate methotrexate (MTX) enantiomers in a run buffer containing chiral 2-hydroxypropyl-β-cyclodextrin [65]. The MTX enantiomers were detected through their dynamic quenching of 1-bromo-4-naphthalene sulfonic acid (BrNS) and the use of TR detection allowed for L-MTX amounts to be determined in a cell culture extract. The detection limits achieved by this method were an order of magnitude better than previous UV absorption techniques.

5.2.2. DNA sequencing by lifetime multiplexing. This application of TR-CE was achieved by attaching dyes with different lifetimes to DNA primers binding to the four different terminal bases of ssDNA [48]. Upon incubation with a fragmented DNA template, CGE separates the fragment-primer duplexes by the length of the fragment and TRF detection indicates the lifetime of the dye-labeled primer, hence the identity of the terminal base. In this way the sequence of a template can be reconstructed.

Lieberwirth et al. did this using four dyes absorbing at 630 nm with lifetimes of 3.7 ns, 2.9 ns, 2.4 ns and 1.6 ns [49]. Linker lengths were used to tune the mobilities of the dye-labeled primers to avoid the need for post-electrophoretic mobility corrections. A pulsed semiconductor laser was used for excitation with a repetition rate of 22 MHz and pulse widths of 500 ps. TCSPC with a SPAD detector provided the TRF data and lifetime values were determined by MLE with 80% accuracy and by a pattern-recognition technique with 90% accuracy. Some dyes exhibited multi-exponential behavior, which contributed to the poor accuracy of MLE. Accuracy of identification was nearly independent of base number and the resolution of CGE allowed for sequencing up to 660 base pairs in one channel. Overlapping peaks, due to the inhomogeneity of the gel matrix or sequence-specific effects, were a source of error. Fig. 3 shows the fluorescence intensity and lifetime data retrieved by this technique for four resolved peaks corresponding to 135, 136, 137 and 138 base pairs.

To improve the throughput of one-lane sequencing, Neumann et al. developed a stage-scanning 16-capillary device that used discontinuous, bidirectional scanning with scan rates near 1 Hz [50]. The IRF of the system and speed of the TCSPC card set the minimum collection time as 150 μs per capillary, but collection times of 10–100 ms were used. Confocal optics were used to creat a detection volume of approximately 500 fL and achieve an LOD of 20–150 molecules in each capillary. DNA template fragments labeled with a single dye-labeled primer were injected into eight capillaries and parallel analysis was successful in seven of the eight. Neumann et al. proposed using the primers designed by Lieberwirth et al. to allow for sequencing of 660 base pairs in eight capillaries, a total of 4800 base pairs.

Lassiter et al. created a TR scanning instrument by moving the optics of the system [26]. With this system, sequencing was done on multiple lanes of slab gels. A SPAD with a large photoactive area (500 μm diameter) and high dark count had to be used for sufficient collection of light, as the moving optics defocused the beam. 400 measurements were made per scan line, with 10-ms acquisition time and 35-μm scanning distance per scan. Sequencing experiments were performed using dyes with lifetimes of 718 ps and 983 ps. The dyes had different mobilities, so post-electrophoresis corrections were necessary. MLE was used to determine lifetimes and errors approached the shot-noise limit. Monte Carlo simulations were used to determine a method of extracting individual lifetimes from overlapping peaks and the instrument was tested using 2-lane/2-dye and 4-lane/1-dye sequencing formats. The 2-lane implementation provided higher accuracy, as lifetime data could be used to distinguish between overlapping fragments. A 670-bp strand of DNA was sequenced with 99.7% accuracy by the 2-lane method and the same template was sequenced with 95.7% accuracy by the 4-lane method.

Spectral and TR DNA sequencing was developed using two pulsed semiconductor lasers with 680 nm and 780 nm emission [28,51]. The IRF of the two channels was 450 ps and 510 ps for the 710-nm and 810-nm channels, respectively. Peaks were identified using software and a single-lifetime measurement was determined at the center of each peak using MLE. Each fragment peak was identified if its lifetime value fell within three

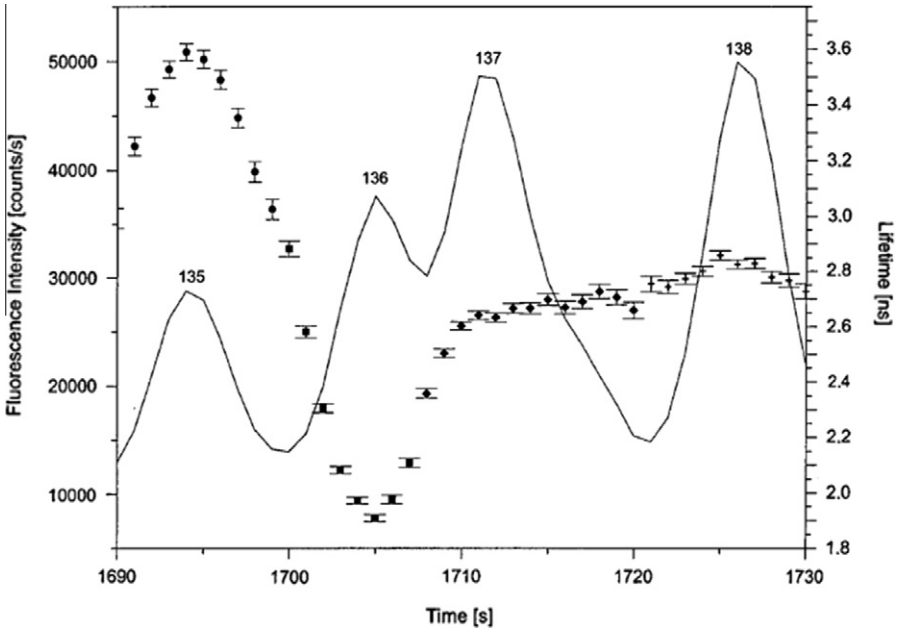

Figure 3. Electropherogram (solid line), fluorescence decay times (symbols), and errors (standard deviation in the decay time determination) of a small part of the sequencing run to illustrate the lifetime distribution inside and between the peaks. The fluorescence decay times were calculated by a MLE algorithms and each peak corresponds to a dye-labeled primer with a different lifetime, hence a different terminal base. Reprinted from [36], with permission from the American Chemical Society.

standard deviations of a premeasured lifetime. If the measured lifetime was not close to any premeasured values, the peak was treated as biexponential decay from overlapping peaks and the lifetime was found by tracking lifetime values from the previous and following peaks. Mobility-shift factors were determined in separate experiments as a function of dye and fragment length and used in data analysis. The lasers were fired alternately to make the channels temporally, as well as spectrally, resolved and zmol LODs were achieved in both channels. For a 650 base pair template, 319 base pairs were analyzed under 680 nm excitation with an accuracy of 96.2% and 331 base pairs were analyzed under 780 nm excitation with an accuracy of 94.0%. The discrepancy in accuracy between channels occurred because the dyes excited at 780 nm excitation were closer in lifetime than the two other dyes. Overall, 95.1% base-calling accuracy was achieved for a 650 base-pair sequence. Stryjewski et al. proposed a two-color, four-lifetime design to sequence a single template in forward and reverse directions.

Llopis, Stryjewski and Soper developed a TR PMMA microchip electrophoresis device [27] using the scanning device and data-analysis methods of Lassiter et al. [26]. Plexiglass was chosen as the material for the microchip, as it contributed little to the IRF and was easy to machine. The two dyes used had lifetimes of 933 ps and 844 ps, but high background and low loading volumes biased measurements towards longer lifetimes. The fitting algorithm was modified to account for the background and the accuracy of lifetime measurements was improved. The high electroosmotic flow of the Plexiglass chip and tailing from solute-Plexiglass interactions prevented single-base resolution on this platform.

Zhu, Stryjewski and Soper created a 7 cm long, 20 μm × 50 μm, single-channel glass microchip to be used for time- and wavelength-resolved separation by gel electrophoresis [32]. Samples were injected in 100-μm plugs by a side-channel and the dimensions of the chip allowed for reduced separation times. The design and data-acquisition method were the same as previous time- and spectral-resolved studies [28,51], but a better objective was used with a higher numerical aperture and reduced chromatic aberrations. Samples were preconcentrated and purified using solid-phase reversible immobilization, and concentration LODs of 3–30 pM were measured. A 294-base strand of DNA was sequenced with 153 bases identified in the 710-nm channel with 90.8% accuracy and 141 bases identified in the 810-nm channel with 83.7% accuracy.

5.2.3. Frequency-domain lifetime determination. Data acquisition for frequency-domain measurements can be performed at millisecond intervals under continuous excitation, so that the speed of separation and the quality of detection are not interrupted [33]. The frequency-domain method was used to determine the lifetimes of two dyes, 1.4 ns and 1 ns, separated in a CE run.

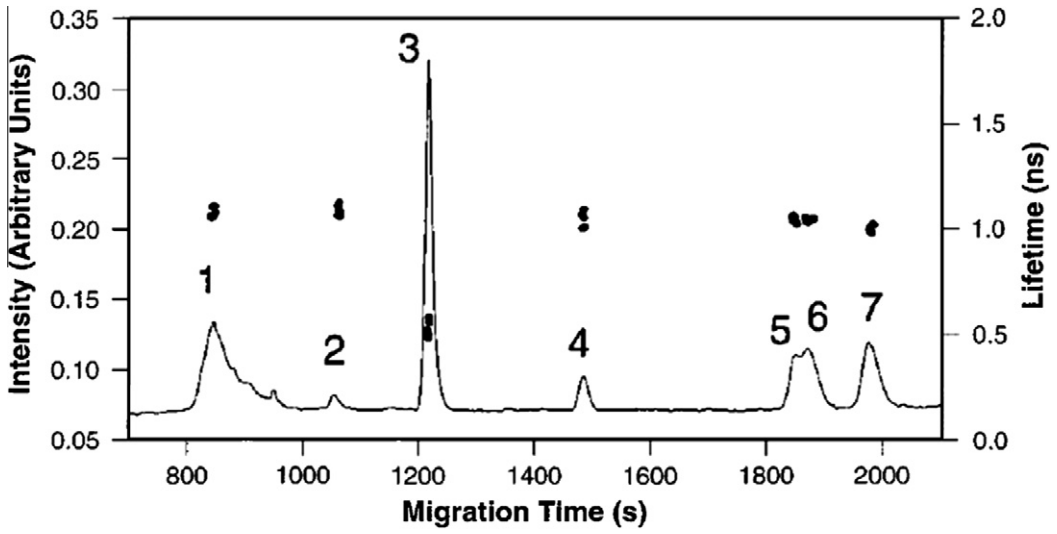

Figure 4. Electropherogram (solid line) and lifetime measurements (points) for a mixture of DNA fragments (peaks 1, 2, 4-7) and a 200 base pair DNA fragment (peak 3) which acts as a reference. Five lifetime points were measured for each peak. Reprinted from [71], with permission from the American Chemical Society.

Nunnally et al. investigated three separate four-dye sets in an attempt to find four dyes to use for DNA sequencing [66]. The best dyes had lifetimes of 1.1 ns, 2.2 ns, 4.3 ns and 5.9 ns and were excited at 488 nm. The lifetimes of the dyes changed when bound to the primer, so only three dyes could be resolved during separation. NLLS was used for lifetime determinations of the dye-labeled primers and the model used for fitting was confirmed by MEM. Lifetime measurements could even be made at the peak edges, where attomole quantities of analyte were expected.

He et al. conducted another study on different four-dye sets [67]. In this study, a method for determining lifetimes of overlapping peaks was developed using NLLS to fit the data to a multi-exponential sum of the four predetermined lifetime values. In addition, a short lifetime value representing the background signal was incorporated into the model. All three four-dye sets proved to be useful for lifetime determination studies on CGE.

Using two dye-labeled primers, He and McGown sequenced a 320 base strand of DNA with an accuracy of 94% [68]. Using NLLS with a multi-exponential decay model, the same template was sequenced with an accuracy greater than 99%. A three dye-labeled primer system was tested using a one-component NLLS decay model and fragments between 51 and 300 bases could be sequenced with an accuracy of 90%. Upon switching to a three-component NLLS model, 320 bases could be sequenced with 97% accuracy. Data smoothing and noise filtering were further used to improve accuracy to 98.5%. To adopt a four-dye system, one dye was chosen as a FRET donor-acceptor pair, but the size of the FRET dye prompted the need for mobility corrections to the data. The lifetimes of the four dyes used were 1.7 ns, 2.5 ns, 2.9 ns and 3.5 ns. A single-component model allowed for sequencing up to 220 bases with 96% accuracy whereas the multiple-component model was unable to identify the fragments.

Several studies were performed with the purpose of optimizing the performance of the frequency-domain technique of lifetime determination. Two studies sought to optimize the gel and sieving buffers used and it was found that lifetime values were affected by the choice of sieving buffer [69] but not the various gel conditions tested [70]. The optical components of the instrument were also optimized, and it was found that, by using a holographic notch filter, a single-lens configuration and by switching to a square capillary, the signal-to-noise ratio of the system could be improved [34].

The frequency-domain technique has also found some use in non-sequencing applications. McIntosh et al. used their system to perform DNA analysis by restriction fragment length polymorphism (RFLP) using lifetime multiplexing [71,72]. In RFLP, a DNA template is cut by a restriction enzyme resulting in a distribution of fragment sizes unique to the template sequence. The fragmented DNA strand was labeled with one intercalating dye and a DNA ladder labeled with another. The two samples were run in the same CGE experiment so that the length of the template fragments could be easily checked against the DNA ladder, shown in Fig. 4.

The frequency-domain CE instrument was also used to study humic substances by CZE [73]. In CE, humic substances tend to migrate as a single peak and the lifetime data provided by frequency-domain measurements gives extra information that can be used to

characterize the contents of the peak. The 364-nm and 488-nm lines of an argon-ion laser were used to measure absorbance and emission spectra for various humic samples and fluorescent lifetime data were determined by NLLS using single- and multi-component models.

Snyder and McGown used lifetime determination to analyze single-strand conformation polymorphisms in order to detect point mutations in DNA [74]. A wild-type template was labeled with a 5-ns-lifetime dye and a DNA strand containing a mutation with a 3-ns-lifetime dye. Both strands were amplified and allowed to form ssDNA secondary structures, then analyzed in the same CE run. Using NLLS with a multi-exponential decay model, the peaks of the two strands were resolved in one run, even if their peaks overlapped.

6. Conclusions

When coupled with electrophoretic methods, TR detection has been used to increase the sensitivity and versatility of measurements, with

(1) LODs of thousands, hundreds and single molecules reported,
(2) improvements made to the analysis of contaminated samples, and
(3) the identification of multiple species in a single run, and on a single spectral channel, by lifetime.

However despite the advantages, TR-CE has not become a widely used technique in analytical chemistry. The use of TR-CE to improve sensitivity is not needed as long as steady-state methods allow for just as good, if not better, sensitivity. While TR-CE showed some novelty as a method for DNA sequencing, the success of other methods has caused research on the subject to be abandoned.

Early TR-CE studies suffered from instrument and reagent-based limitations. The lasers possessed pulse widths that were too long, unstable over time, or of lower intensity than cw sources. High intensity, stable, sub-ps pulses were achievable, but only with expensive and complex Ti:sapphire lasers. Detector technology also posed a problem, as equipment necessary for TCSPC had to be purchased and assembled piece by piece. Also, the lack of high-quality dyes that could be used under standard CE, or CGE, conditions made progress more difficult.

However, today, commercial solutions exist for many of these issues. Pulsed laser diodes, low dark-count SPADs and integrated TCSPC PC boards are easy to obtain and to operate. Organic dyes with good photophysical properties are available for most laser lines. Numerous books and publications on TR instrumentation, design and experimental methodology are also available.

This review has shown that TR detection on CE is an achievable and versatile analytical technique with the potential to provide a variety of improvements to the CE platform. However, TR-CE suffers from a lack of relevant experimental methodology, which means that the cost of TR instrumentation outweighs its benefits. For successful implementation of a TR-CE instrument, focus must be placed on developing experimental methods that can make sufficient gains from it.

Acknowledgements

This work was supported by NSERC Canada. The authors thank Victor Galievsky for reading the manuscript and providing critical comment.

References

[1] V. Okhonin, M. Berezovski, S.N. Krylov, J. Am. Chem. Soc. 124 (2004) 7166.
[2] M. Berezovski, S.N. Krylov, J. Am. Chem. Soc. 124 (2002) 13674.
[3] A. Petrov, V. Okhonin, M. Berezovski, S.N. Krylov, J. Am. Chem. Soc. 127 (2005) 17104.
[4] V. Okhonin, A. Petrov, M. Berezovski, S.N. Krylov, Anal. Chem. 78 (2006) 4803.
[5] A.P. Petrov, L.T. Cherney, B. Dodgson, V. Okhonin, S.N. Krylov, J. Am. Chem. Soc. 133 (2011) 12486.
[6] M. Berezovski, A. Drabovich, S.M. Krylova, M. Musheev, V. Okhonin, A. Petrov, S.N. Krylov, J. Am. Chem. Soc. 127 (2005) 3165.
[7] A. Drabovich, M. Berezovski, S.N. Krylov, J. Am. Chem. Soc. 127 (2005) 11224.
[8] M. Berezovski, M. Musheev, A. Drabovich, S.N. Krylov, J. Am. Chem. Soc. 128 (2006) 1410.
[9] A.P. Drabovich, M. Berezovski, V. Okhonin, S.N. Krylov, Anal. Chem. 78 (2006) 3171.
[10] S.N. Arkhipov, M. Berezovski, J. Jitkova, S.N. Krylov, Cytometry 63 (2005) 41.
[11] B. Davis, Scientist 19 (2005) 27.
[12] S.N. Krylov, E. Arriaga, Z. Zhang, N.W.C. Chan, M.M. Palcic, N.J. Dovichi, Cytometry 37 (1999) 14.
[13] R.T. Kennedy, M.D. Oates, B.R. Cooper, B. Nickerson, J. Jorgenson, Science (Washington, DC) 246 (1989) 57.
[14] V. Okhonin, X. Liu, S.N. Krylov, Anal. Chem. 77 (2005) 5925.
[15] E. Wong, V. Okhonin, M.V. Berezovski, T. Nozaki, H. Waldmann, K. Alexandrov, S.N. Krylov, J. Am. Chem. Soc. 130 (2008) 11862.
[16] S.M. Krylova, V. Okhonin, C.J. Evenhuis, S.N. Krylov, Trends Anal. Chem. 28 (2009) 987.
[17] A.P. Petrov, B.J. Dodgson, L.T. Cherney, S.N. Krylov, Chem. Comm. 47 (2011) 7767.
[18] K. Swinney, D.J. Bishop, Electrophoresis 21 (2000) 1239.
[19] D.Y. Chen, N.J. Dovichi, J. Chromatogr., B 657 (1994) 265.
[20] J.A. Taylor, E.A. Yeung, Anal. Chem. 65 (1993) 956.
[21] Y.F. Cheng, S. Wu, D.Y. Chen, N.J. Dovichi, Anal. Chem. 62 (1990) 496.
[22] E. Waddell, S. Lassiter, C.V. Owens Jr., S.A. Soper, J. Liq. Chromatogr. Relat. Technol. 23 (2000) 1139.
[23] I. Hyppanen, T. Soukka, J. Kankare, J. Phys. Chem. A 114 (2010) 7856.
[24] C.M. McGraw, G. Khalil, J.B. Callis, J. Phys. Chem. C 112 (2008) 8079.
[25] J.R. Lakowicz. Principles of Fluorescence Spectroscopy, Third Edition, Springer Science + Business Media, LLC, New York, USA, 2006.
[26] S.J. Lassiter, W. Stryjewski, B.L. Legendre Jr., R. Erdmann, M. Wahl, J. Wurm, R. Peterson, L. Middendorf, S.A. Soper, Anal. Chem. 72 (2000) 5373.

[27] S.D. Llopis, W. Stryjewski, S.A. Soper, Electrophoresis 25 (2004) 3810.
[28] W.J. Stryjewski, S.A. Soper, S. Lassiter, L. Davis, in: D.J. Bornhop, D.A. Dunn, R.P. Mariella Jr., C.J. Murphy (Editors), Biomedical Nanotechnology Architectures and Applications, Proc. SPIE 4626 (2002) p. 201.
[29] J.B. Pawley, Handbook of Biological Confocal Microscopy, Springer Science + Business Media, LLC, New York, USA, 2006.
[30] C. Zander, K.H. Drexhage, K.T. Han, J. Wolfrum, M. Sauer, Chem. Phys. Lett. 286 (1998) 457.
[31] S. Hillebrand, J.R. Schoffen, M. Mandaji, C. Termignoni, H.P.H. Grieneisen, T.B.L. Kist, Electrophoresis 23 (2002) 2445.
[32] L. Zhu, W.J. Stryjewski, S.A. Soper, Anal. Biochem. 330 (2004) 206.
[33] L. Li, L.B. McGown, Anal. Chem. 68 (1996) 2737.
[34] L. Li, L.B. McGown, Electrophoresis 21 (2000) 1300.
[35] A. Fultz, T.M. Branch, V. Majidi, Microchem. J. 57 (1997) 231.
[36] S.A. Soper, B.L. Legendre Jr., D.C. Williams, Anal. Chem. 67 (1995) 4358.
[37] G. Bachteler, K.H. Drexhage, J. Arden-Jacob, K.T. Han, M. Köllner, R. Müller, M. Sauer, S. Seeger, J. Wolfrum, J. Lumin. 62 (1994) 101.
[38] J. Tellinghuisen, C.W. Wilkerson Jr., Anal. Chem. 65 (1993) 1240.
[39] P. Hall, B. Selinger, J. Phys. Chem. 85 (1981) 2941.
[40] M. Maus, M. Cotlet, J. Hofkens, T. Gensch, F.C. De Schryver, J. Schaffer, C.A.M. Seidel, Anal. Chem. 73 (2001) 2078.
[41] K.J. Miller, F.E. Lytle, J. Chromatogr. 648 (1993) 245.
[42] K.J. Miller, I. Leesong, J. Bao, F.E. Regnier, F.E. Lytle, Anal. Chem. 65 (1993) 3267.
[43] B.L. Legendre Jr., S.A. Soper, Appl. Spectrosc. 50 (1996) 1196.
[44] M. Latva, T. Ala-Kleme, H. Bjennes, J. Kankare, K. Haapakka, Analyst (Cambridge, UK) 120 (1995) 367.
[45] S.J. Kok, I.C.K. Isberg, C. Gooijer, U.A. Brinkman, N.H. Velthorst, Anal. Chim. Acta 360 (1998) 109.
[46] G.K. Belin, S. Seeger, J. Nanosci. Nanotechnol. 9 (2009) 2645.
[47] J.M. Song, H. Kawazumi, T. Inoue, T. Ogawa, J. Chromatogr., A 727 (1996) 330.
[48] M. Sauer, J. Arden-Jacob, K.H. Drexhage, N.J. Marx, A.E. Karger, U. Lieberwirth, R. Müler, M. Neumann, S. Nord, A. Paulus, A. Schulz, S. Seeger, C. Zander, J. Wolfrum, Biomed. Chromatogr. 11 (1997) 81.
[49] U. Lieberwirth, J. Arden-Jacob, K.H. Drexhage, D.P. Herten, R. Müller, M. Neumann, A. Schultz, S. Siebert, G. Sagner, S. Klingel, M. Sauer, J. Wolfrum, Anal. Chem. 70 (1998) 4771.
[50] M. Neumann, D.P. Herten, A. Dietrich, J. Wolfrum, M. Sauer, J. Chromatogr., A 871 (2000) 299.
[51] L. Zhu, W. Stryjewski, S. Lassiter, S.A. Soper, Anal. Chem. 75 (2003) 2280.
[52] I. Lammers, J. Buijs, G. van der Zwan, F. Ariese, C. Gooijer, Anal. Chem. 81 (2009) 6226.
[53] M.W.F. Nielsen, J. Chromatogr. 608 (1992) 85.
[54] K. Sumitomo, T. Ito, M. Sasaki, Y. Yamaguchi, Chromatographia 67 (2008) 715.
[55] Y. Yamaguchi, K. Hashino, M. Ito, K. Ikawa, T. Nishioka, K. Matsumoto, Anal. Sci. 25 (2009) 327.
[56] Hamamatsu, Photomultiplier Tubes: Basics and Applications, Third Edition, Hamamatsu Photonics K.K., Hamamatsu City, Japan, 2007.
[57] Perkin Elmer, Avalanche Photodiodes: A User's Guide, Perkin Elmer Inc. 2007 (http://www.bgu.ac.il/~glevi/website/Guides/AvalanchePhotodiodes.pdf).
[58] W. Becker, Advanced Time Correlated Single Photon Counting Techniques, Springer Science + Business Media, Berlin, Germany, 2005.
[59] B.L. Legendre Jr., D.C. Williams, S.A. Soper, R. Erdmann, U. Ortmann, J. Enderlein, Rev. Sci. Instrum. 67 (1996) 3984.
[60] L.M. Smith, J.Z. Sander, R.J. Kaiser, P. Hughes, C. Dodd, C.R. Connell, C. Heiner, S.B.H. Kent, L.E. Hood, Nature (London) 321 (1986) 674.
[61] J. Ju, C. Ruan, C.W. Fuller, A.N. Glazer, R.A. Mathies, Proc. Natl. Acad. Sci. USA 92 (1995) 4347.
[62] J. Ju, A.N. Glazer, R.A. Mathies, Nat. Med. 2 (1996) 246.
[63] M. Castro-Puyana, I. Lammers, J. Buijs, C. Gooijer, F. Ariese, Electrophoresis 31 (2010) 3928.
[64] I. Lammers, J. Buijs, F. Ariese, C. Gooijer, Anal. Chem. 82 (2010) 9410.
[65] M. Castro-Puyana, I. Lammers, J. Buijs, C. Gooijer, F. Ariese, Anal. Bioanal. Chem. 400 (2011) 2913.
[66] B.K. Nunnally, H. He, L. Li, S.A. Tucker, L.B. McGown, Anal. Chem. 69 (1997) 2392.
[67] H. He, B.K. Nunnally, L. Li, L.B. McGown, Anal. Chem. 70 (1998) 3413.
[68] H. He, L.B. McGown, Anal. Chem. 72 (2000) 5865.
[69] L. Li, L.B. McGown, Fresenius' J. Anal. Chem. 369 (2001) 267.
[70] L. Li, L.B. McGown, J. Chromatogr., A 841 (1995) 95.
[71] S.L. McIntosh, B.K. Nunnally, A.R. Nesbit, T.G. Deligeorgiev, N.I. Gadjev, L.B. McGown, Anal. Chem. 72 (2000) 5444.
[72] S.L. McIntosh, T.G. Deligeorgiev, N.I. Gadjev, L.B. McGown, Electrophoresis 23 (2002) 1473.
[73] J.D. Hewitt, L.B. McGown, Appl. Spectrosc. 57 (2003) 256.
[74] T.M. Snyder, L.B. McGown, Appl. Spectrosc. 59 (2005) 335.